Pancreatic exocrine insufficiency in LXR$\beta^{-/-}$ mice is associated with a reduction in aquaporin-1 expression

Chiara Gabbi*, Hyun-Jin Kim*, Kjell Hultenby†, Didier Bouton*, Gudrun Toresson*, Margaret Warner*, and Jan-Åke Gustafsson*‡

*Department of Biosciences and Nutrition, †Clinical Research Center, Karolinska Institutet, Novum, S-141 86, Stockholm, Sweden

Contributed by Jan-Åke Gustafsson, August 15, 2008 (sent for review July 18, 2008)

Liver X receptors (LXRs) α and β are nuclear oxysterol receptors with a key role in cholesterol, triglyceride, and glucose metabolism. In LXR$\beta^{-/-}$ mice on a normal diet, there is a reduction in size of perigonadal fat pad and, on high-fat diet there is resistance to obesity. In the present study, we investigated the reason for the resistance of LXR$\beta^{-/-}$ mice to weight gain. In LXR$\beta^{-/-}$ mice we found pancreatic exocrine insufficiency with reduced serum levels of amylase and lipase, reduced proteolytic activity in feces, chronic inflammatory infiltration, and, in the ductal epithelium, an increased apoptosis without compensatory proliferation. Electron microscopy revealed ductal dilatation with intraductal laminar structures characteristic of cystic fibrosis. To investigate the relationship between LXRβ and pancreatic secretion, we studied the expression of LXRβ and the water channel, aquaporin-1 (AQP1), in the ductal epithelium of the pancreas. In WT mice, ductal epithelial cells expressed LXRβ in the nuclei and AQP1 on the plasma membrane. In LXR$\beta^{-/-}$ mice neither LXRβ nor AQP1 was detectable. Moreover, in WT mice the LXR agonist (T2320) increased AQP1 gene expression. These data demonstrate that in LXR$\beta^{-/-}$ mice dietary resistance to weight gain is caused by pancreatic insufficiency and that LXRβ regulates pancreatic exocrine secretion through the control of AQP1 expression. Pancreatic exocrine insufficiency is the main cause of malabsorption syndrome responsible for weight loss in adults and growth failure in children. Several genes are known to be involved in the pathogenesis and susceptibility to pancreatic insufficiency. LXRβ should be included in that list.

pancreas | malabsorption | cystic fibrosis | amylase | lipase

Malabsorption syndrome is a clinical condition characterized by a combination of symptoms like weight loss or growth failure in children, steatorrhea, diarrhea, and anemia that result from unsuccessful nutrient absorption from the diet. Numerous diseases are responsible for this syndrome, and according to their etiology, they can be classified into three groups: (*i*) alterations of the digestive process caused by deficit of enzymes and bile acids such as in chronic pancreatitis, cystic fibrosis, and cholestatic liver diseases; (*ii*) alterations in uptake and transport caused by a damage of absorptive surface such as in celiac disease, Crohn's disease, and autoimmune enteropathy; and (*iii*) microbial causes such as bacterial overgrowth and parasitosis (1). The major cause of defective intraluminal digestion is pancreatic exocrine insufficiency caused by chronic pancreatitis and cystic fibrosis. In industrialized countries, the incidence of chronic pancreatitis is between 3.5 and 10 per 100,000 inhabitants. About 70–80% of cases are related to long-term alcohol misuse, whereas 10–30% of cases represent idiopathic pancreatitis for which the etiology is still unknown (2). A large number of mutations in genes coding for serine protease inhibitor, SPINK1, or the cystic fibrosis transmembrane conductance regulator, CFTR, have been described to be involved not only in the pathogenesis of pancreatitis but also, working in concert with other genetic and environmental factors, in the susceptibility to this disease (3). Moreover, in humans, it has been shown that genetic polymorphisms of genes regulating the inflammatory response, like heat shock protein 70-2 or tumor necrosis factor α, are associated with an increased risk of acute pancreatitis (4).

Liver X receptors, LXRα (NR1H3) and LXRβ (NR1H2), are nuclear receptors belonging to the superfamily of ligand-activated transcription factors with a key role in controlling lipid and glucose metabolism. Ligands for LXRs are 22-hydroxycholesterol, 24(S)-hydroxycholesterol, 24(S),25-epoxycholesterol, and 27-hydroxycholesterol that at physiological concentrations bind to and activate these receptors (5). Recently, high concentrations of glucose and D-glucose were reported to be activators of LXRs (6). Whereas high levels of LXRα mRNA are expressed in liver, adipose tissue, adrenal glands, intestine, kidney, macrophages, and lung, LXRβ mRNA is widely distributed through the body with high levels in the developing brain (7, 8). LXRs form obligate heterodimers with retinoid X receptor (RXR). The complex LXR/RXR that can be activated by ligands of either partner bind to LXR-responsive elements (LXREs) consisting of a direct repeat (DR4) of the sequence 5′-AGGTCA-3′ separated by 4 nt on the promoter of target genes. LXR target genes are involved in cholesterol transport in liver [ATP-binding cassette transporter (ABC) G5, ABCG8] and macrophages (ABCG1, ABCG4, ABCA1), fatty acid and triglyceride synthesis (fatty acids synthase, acetyl-Coenzyme A carboxylase, stearoyl-Coenzyme A desaturase 1, sterol regulatory element binding transcription factor), bile acid metabolism (cholesterol 7-α-hydroxylase), and glucose homeostasis (phosphoenolpyruvate carboxykinase, glucose-6-phosphatase) (9).

Studies of LXR knockout mice during a fat diet challenge have revealed that the two isoforms, despite their very high sequence homology (78%), have distinct physiological roles in the body. LXR$\alpha^{-/-}$ mice, fed a diet supplemented with 2% cholesterol, accumulate cholesterol in the liver whereas LXR$\beta^{-/-}$ mice are resistant to cholesterol accumulation (10, 11). In male LXR$\beta^{-/-}$ and LXR$\alpha^{-/-}\beta^{-/-}$ on a normal diet, the gonadal fat pad is reduced with a decrease in adipocyte size and when fed with a high-fat diet, they are resistant to obesity (12). Moreover, LXR$\alpha^{-/-}\beta^{-/-}$ mice do not gain weight when fed with a diet containing both high fat and cholesterol (13).

In the present study we demonstrate that LXR$\beta^{-/-}$ mice at 11 months of age on a standard diet exhibit a pancreatic exocrine insufficiency that may be responsible for the described resistance of these mice to gain weight. With specific antibodies we show that both LXRβ and the water channel aquaporin-1 (AQP1) are expressed in the epithelial cells of the pancreatic ducts in WT mice and that ductal expression of AQP1 is markedly reduced in LXR$\beta^{-/-}$ mice. This reduction is likely responsible for the dense secretory fluid in the exocrine pancreas of LXR$\beta^{-/-}$ mice

Author contributions: C.G., M.W., and J.- Å.G. designed research; C.G. and H.-J.K. performed research; C.G., K.H., D.B., G.T., and M.W. contributed new reagents/analytic tools; C.G. analyzed data; and C.G., M.W., and J.- Å.G. wrote the paper.

Conflict of interest statement: J.-Å.G. is a shareholder and consultant of KaroBio AB.

‡To whom correspondence should be addressed. E-mail: jan-ake.gustafsson@ki.se.

www.pnas.org/cgi/doi/10.1073/pnas.0808097105

Table 1. Anthropometric parameters in 11-month-old male and female mice

Parameter	WT	LXR$\alpha^{-/-}$	LXR$\beta^{-/-}$	LXR$\alpha^{-/-}\beta^{-/-}$
Male mice				
Number	4	4	4	3
Body weight, g	48.22 ± 2.54	46.8 ± 3.46	36.7 ± 1.96*	33.58 ± 0.87*
Nasoanal length, cm	11.78 ± 0.15	11.05 ± 0.37	11.47 ± 0.1	10.17 ± 0.29*
Weight (g)/length (cm) ratio	4.09 ± 0.19	4.24 ± 0.33	3.2 ± 0.15*	3.3 ± 0.06*
Perigonadal fat, g	2.18 ± 0.23	1.92 ± 0.62	0.91 ± 0.28*	0.4 ± 0.04*
Perigonadal fat/body weight, %	4.5 ± 0.76	4.04 ± 0.96	2.41 ± 0.63*	1.2 ± 0.08*
Caloric intake, KJ/g body weight per day	2.03 ± 0.28	1.89 ± 0.09	2.27 ± 0.2	2.35 ± 0.15
Female mice				
Number	5	4	3	5
Body weight, g	36.19 ± 1.24	31.49 ± 1.59	25.62 ± 0.37*	26.54 ± 0.79**
Nasoanal length, cm	10.66 ± 0.19	10.25 ± 0.14	9.5 ± 0.01*	9.46 ± 0.16*
Weight (g)/length (cm) ratio	3.4 ± 0.15	3.07 ± 0.17	2.7 ± 0.4**	2.8 ± 0.05**
Perigonadal fat, g	1.68 ± 0.12	1 ± 0.13*	0.33 ± 0.08**	0.32 ± 0.02**
Perigonadal fat/body weight, %	4.6 ± 0.5	3.15 ± 0.26*	1.29 ± 0.55*	1.22 ± 0.08**
Caloric intake, KJ/g body weight per day	1.88 ± 0.09	2.1 ± 0.18	2.24±0.03*	2.15 ± 0.07

Data are presented as mean ± SEM. *, $P < 0.05$; **, $P < 0.001$ versus WT. Food intake and body weight were measured daily for 7 days in mice at 11 months of age.

visualized by electron microscopy and for the pancreatic insufficiency. In WT mice, 7 days of treatment with an LXR agonist (T2023) significantly increased mRNA levels of AQP1 in WT mice. These findings suggest that LXRβ plays an important role in controlling pancreatic juice secretion through the regulation of water transport.

Results

Decreased Body Weight and Perigonadal Fat Pad in LXR$\beta^{-/-}$ Mice. As shown in Table 1, at 11 months of age, both male and female LXR$\beta^{-/-}$ mice had significantly lower body weights, weight/length ratios, and perigonadal fat pad size than WT mice. Interestingly, the same phenotype was also evident in LXR$\alpha^{-/-}\beta^{-/-}$ mice but not in LXR$\alpha^{-/-}$ mice, confirming a specific role for LXRβ in the control of body weight.

In 11-month-old male mice, the caloric intake monitored for 1 week was not different among the four genotypes, whereas a significant increase was detected in LXR$\beta^{-/-}$ female mice. Despite the augmented caloric intake, female LXR$\beta^{-/-}$ mice showed a reduced weight, similar to male LXR$\beta^{-/-}$ mice.

Interestingly, even though there was no difference in body weight between LXR$\alpha^{-/-}$ and WT female mice, the perigonadal fat pad was much smaller in the LXR$\alpha^{-/-}$mice, indicating that in these mice there is perhaps fat accumulation in another tissue, probably the liver.

Pancreatic Exocrine Insufficiency in LXR$\beta^{-/-}$ Mice. Serum levels of lipase and α-amylase were significantly decreased in both male and female LXR$\beta^{-/-}$ mice, indicating a reduction in secretion of pancreatic enzymes (Fig. 1 *A* and *B*).

The pancreas secretes a large amount of digestive proteases into the gut. The activity of total proteases in feces was measured by using Azo-casein as a substrate. There was a significant reduction in the proteolytic activity in the feces of both male and female LXR$\beta^{-/-}$ mice and in LXR$\alpha^{-/-}\beta^{-/-}$ female mice (Fig. 1*C*).

These data constitute supportive evidence of a pancreatic exocrine insufficiency in LXR$\beta^{-/-}$ mice.

Inflammatory Infiltrate with Increased Cell Death in Pancreas of LXR$\beta^{-/-}$ Mice. Morphological examination of pancreatic sections stained with hematoxylin-eosin (Fig. 2 *A* and *B*) showed the presence of periductal inflammatory infiltrates around large and medium-sized pancreatic ducts, as described in duct destructive chronic pancreatitis in humans (14).

Apoptotic cell death was evaluated with TUNEL staining (Fig. 2 *C* and *D*). An increased number of apoptotic cells was evident in the pancreatic ductal epithelia of LXR$\beta^{-/-}$ mice.

Interestingly, there was no significant difference in the number of proliferating ductal cells between WT and LXR$\beta^{-/-}$ mice, suggesting that there was no compensatory increase in proliferation to offset the increased apoptosis in LXR$\beta^{-/-}$ mice (Fig. 2 *E* and *F*). The same morphology was also evident in male mice (data not shown).

Dilatation of Pancreatic Ducts and Cisternae of Golgi in LXR$\beta^{-/-}$ Male Mice. Electron microscopic studies of the pancreas (Fig. 3 *A* and *B*) revealed dilatation of the ducts with dense intraductal material, including laminar structures commonly seen in cystic fibrosis. These findings indicate a highly concentrated pancreatic fluid in LXR$\beta^{-/-}$ mice. Cisternae of the Golgi apparatus were enlarged in LXR$\beta^{-/-}$ mice (Fig. 3 *C* and *D*). These ultrastructural alterations of the Golgi are characteristic of when ATP deficiency occurs during pancreatitis (15).

LXRβ Is Expressed in the Nuclear Region of Pancreatic Duct Epithelial Cells. Anti-LXRβ antibody developed in our laboratory was used to study LXRβ localization in pancreas with immunohistochemistry and Western blotting. Positive staining was detectable in the nuclei of epithelial cells of pancreatic ducts (Fig. 4*A*). Two controls were used to test the specificity of the antibody: first, the positive staining was not evident in pancreas of LXR$\beta^{-/-}$ mice (Fig. 4*C*); second, after preadsorption of the antibody with LXRβ protein the staining in pancreas was negative (Fig. 4*B*).

To confirm the presence of LXRβ in the pancreas, nuclear fractions isolated from WT, LXR$\beta^{-/-}$, and LXR$\alpha^{-/-}\beta^{-/-}$ mice were evaluated by Western blotting (Fig. 4*D*). A band of 56 kDa at the same molecular mass as LXRβ protein standard was detectable in WT extracts but not in LXR$\beta^{-/-}$ mouse extracts.

AQP1 mRNA and Protein Levels Are Reduced in LXR$\beta^{-/-}$ Mice. AQP1 is a water channel expressed in epithelial cells of pancreatic ducts with a key role in transmembrane water movement. To investigate the ethiopathogenesis of the dense secretory fluid in LXR$\beta^{-/-}$ mice, AQP1 gene expression was evaluated by real-time RT-PCR and protein localization with immunohistochemistry. In both LXR$\beta^{-/-}$ male and female mice, the level of AQP-1 mRNA was lower than in WT littermates (Fig. 5*A*). This decrease was much more clearly evident in immunohistochem-

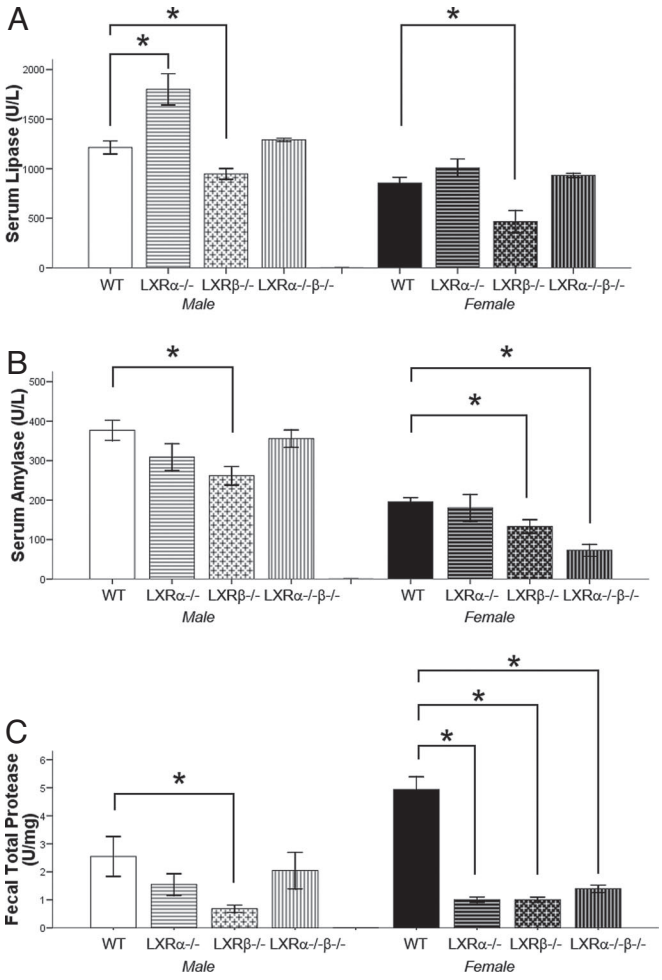

Fig. 1. Serum lipase, α-amylase, and fecal total protease in 11-month-old male and female mice. (*A* and *B*) Levels of lipase (U/l) (*A*) and α-amylase (U/l) (*B*) in serum are significantly lower in LXR$\beta^{-/-}$ male and female mice than in WT mice. LXR$\alpha^{-/-}\beta^{-/-}$ serum α-amylase but not lipase is reduced. (*C*) Total proteases (units/mg) in feces are lower in male LXR$\beta^{-/-}$ mice and female mice of all of the knockout genotypes. Data represent the mean ± SEM. *, $P < 0.05$ versus WT.

istry: in WT mice AQP1 was detectable on the luminal membrane of epithelial cells of pancreatic ducts, whereas in LXR$\beta^{-/-}$ female mice AQP1 was almost undetectable in pancreatic ducts but still evident in endothelia of small blood vessels (Fig. 5*C*). The same reduction was found in male mice (data not shown). The reason for the remaining relatively high levels of AQP-1 mRNA in LXR$\beta^{-/-}$ mice is the high levels of expression of this gene in the vascular system (16, 17). Clearly small blood vessels are abundant in the pancreas and in LXR$\beta^{-/-}$ mice they still express high levels of AQP-1. The data suggest that LXRβ specifically regulates AQP-1 in the ductal epithelium of the pancreas.

AQP1 Expression Is Induced After LXR Agonist Treatment. To evaluate the possibility that AQP-1 could be a target gene of LXRβ, 8-month-old WT male mice were treated with the LXR agonist T2320 for 7 days. AQP-1 expression was studied by RT-PCR (Fig. 6). After treatment with T2320, levels of AQP-1 mRNA were significantly higher than those in vehicle-treated mice, indicating that AQP-1 expression is regulated by LXRβ.

Discussion

In this study we show that in male and female LXR$\beta^{-/-}$ mice at 11 months of age there is pancreatic exocrine insufficiency that

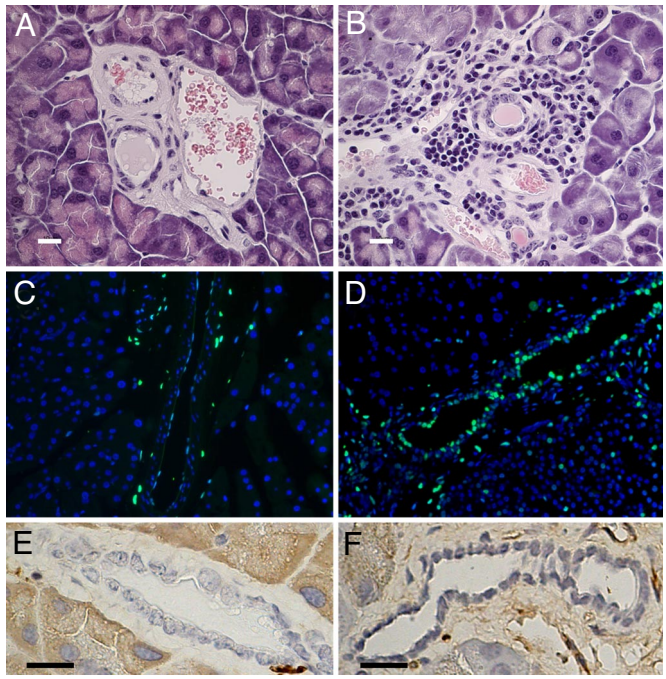

Fig. 2. Immuno-morphological study of 11-month-old female pancreas. (*A* and *B*) Hematoxylin-eosin staining demonstrates a large infiltration of immune cells all around medium-sized pancreatic ducts of LXR$\beta^{-/-}$ mice (*B*) compared with WT mice (*A*). (*C* and *D*) TUNEL staining (green) shows more apoptotic epithelial cells in the pancreatic ducts in LXR$\beta^{-/-}$ mice (*D*) than in WT mice (*C*). Nuclei are counterstained with DAPI. (*E* and *F*) There are no detectable differences between WT mice (*E*) and LXR$\beta^{-/-}$ mice (*F*) in BrdU-positive cells in pancreatic ducts. (Scale bars: 10 μm.)

is most likely responsible for the resistance of these mice to weight gain when they are fed a high-fat diet and for their lower body weight on a standard diet (10, 11).

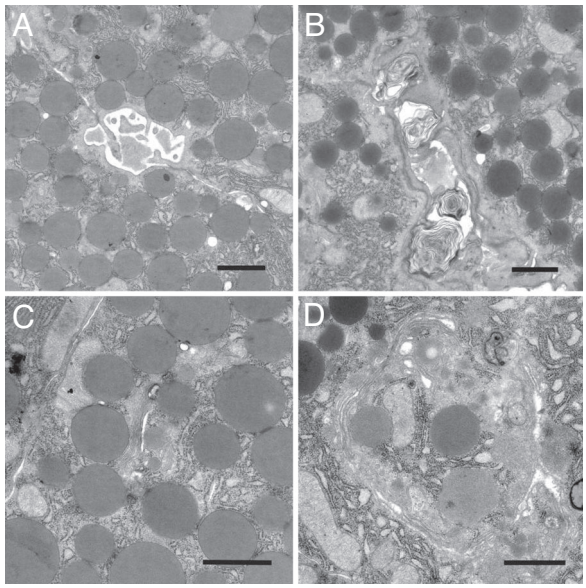

Fig. 3. Pancreatic electron microscopy study of 11-month-old male mice. (*A* and *B*) Laminar structures, characteristic of sticky secretions in luminal region of pancreatic ducts, are detectable in LXR$\beta^{-/-}$ mice (*B*) where a dilatation of the ducts is also evident compared with WT mice (*A*). (*C* and *D*) Cisternae of Golgi apparatus are more dilated in LXR$\beta^{-/-}$ mice (*D*) than in WT mice (*C*). (Scale bars: 1 μm.)

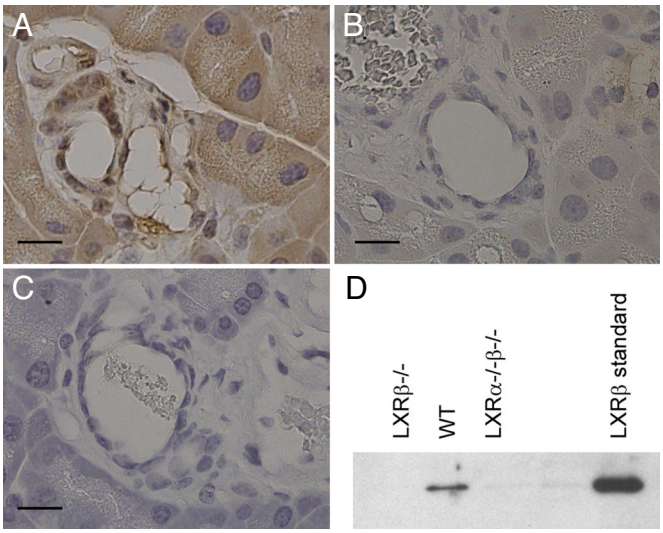

Fig. 4. Study of LXRβ localization in pancreatic ducts. (*A*) LXRβ-positive immunoreactivity is detectable in the nuclear region of pancreatic ductal epithelial cells. (*B* and *C*) The staining is eliminated after preadsorption of the antibody with LXRβ protein (*B*), and there is no nuclear staining in the ductal cells of LXR$\beta^{-/-}$ mice (*C*). (*D*) Nuclear fractions isolated from WT, LXR$\beta^{-/-}$ mice and LXR$\alpha^{-/-}\beta^{-/-}$ mice were examined on Western blots probed with LXRβ antibody. A band of 56 kDa, the same molecular mass as the LXRβ standard protein, is detectable in WT mice but not in LXR$\beta^{-/-}$ or LXR$\alpha^{-/-}\beta^{-/-}$ mice. (Scale bars: 10 μm.)

As demonstrated by low pancreatic enzymes in serum, low levels of total protease in the feces (Fig. 1), massive inflammatory reaction with increased cell death of ductal epithelial cells (Fig. 2), and obstruction with dense material in the intralobular

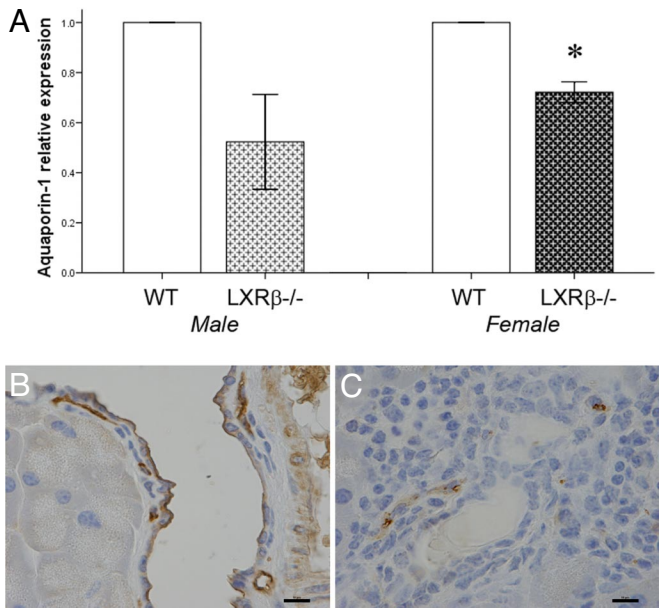

Fig. 5. Expression of AQP1 in pancreas of WT and LXR$\beta^{-/-}$ mice. (*A*) mRNA levels of AQP-1 are significantly decreased in 11-month-old LXR$\beta^{-/-}$ female mice. Values of WT mice were taken as 1, and the knockout mouse values are expressed relative to WT mice. Data represent the mean $\pm$ SE. *, $P < 0.05$ versus WT. (*B* and *C*) Protein levels detected with immunohistochemistry are markedly reduced in pancreatic ducts of LXR$\beta^{-/-}$ female mice (*C*) compared with WT mice (*B*). Positive staining is detectable on the luminal membrane of ductal epithelial cells in WT mice. Staining of AQP-1 in endothelial cells of small blood vessels is still detectable in the knockout animal. (Scale bars: 10 μm.)

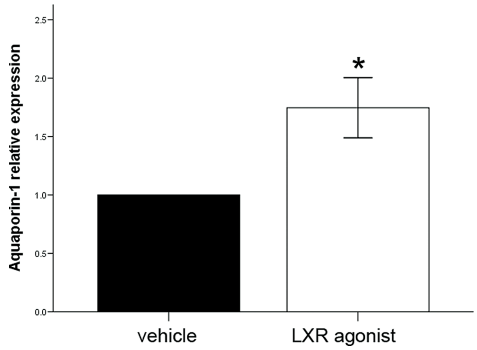

Fig. 6. AQP1 mRNA levels after LXR agonist treatment. After 7 days of LXR agonist (T2320 Sigma–Aldrich) treatment (20 mg/kg), AQP1 mRNA relative expression, quantified with real-time RT-PCR, is significantly increased. Values of vehicle-treated mice were taken as 1, and T2320-treated mouse values are expressed relative to vehicle. Data represent the mean $\pm$ SE. *, $P < 0.05$ versus vehicle.

ducts (Fig. 3), pancreatic exocrine function in LXR$\beta^{-/-}$ mice is severely affected. With a specific antibody directed against LXRβ, we demonstrated the expression of this nuclear receptor in the nuclei of pancreatic ductal epithelial cells (Fig. 4). Staining was eliminated after preadsorption of the antibody with LXRβ protein and no staining was detected in pancreatic sections of LXR$\beta^{-/-}$ mice. The cause of the dense pancreatic secretion appears to be the loss of the water transporter AQP-1 protein in LXR$\beta^{-/-}$ mouse pancreatic ducts (Fig. 5). The resulting alteration in the composition of pancreatic juice is likely responsible for the apoptotic death of the ductal cells and finally pancreatic insufficiency.

AQP-1 is a membrane water channel protein with a key role in transcellular fluid transport. First identified (17) in erythrocytes and renal proximal tubules, it is also expressed in the digestive system, in particular in endothelial cells of capillaries, small vessels, and lymphatic capillaries of the small intestine (16), in cholangiocytes of liver, bile ducts (18), and gallbladder (19), and in the interintra lobular pancreatic ducts (20) where it seems to participate in bile and pancreatic juice formation. Besides an impaired ability to concentrate urine (21, 22), reduced cerebrospinal fluid production (23), defective angiogenesis and cell migration (24), and reduced corneal permeability (25), transgenic mice lacking AQP-1 exhibit one other very interesting metabolic phenotype: on standard chow diet, AQP-1$^{-/-}$ mice show a mild growth retardation (21) and, when fed a high-fat diet, they are resistant to weight gain, develop steatorrhea, and have a decreased concentration of amylase and lipase in pancreatic fluid (26), i.e., a phenotype very similar to that of LXR$\beta^{-/-}$ mice (10–12). Interestingly, in AQP-1$^{-/-}$ mice the rate of pancreatic fluid secretion was not affected but composition studies demonstrated lower enzymatic activity of amylase and lipase (26). It seems that a defective secretion of water in the intrainterlobular pancreatic ducts leads to a modification in the composition of pancreatic secretion.

Recently, an interesting localization of AQP-1 has been demonstrated on the membrane of pancreatic zymogen granules and other secretory vesicles (27–29). After stimulation with GTP, AQP-1 rapidly increases the entry of water into the granules, leading to swelling, a key step in exocytosis (28). Although with immunohistochemistry we did not detect AQP-1 on zymogen granules in our sections, we can suppose that in LXR$\beta^{-/-}$ mice an impaired zymogen granule secretion could occur and participate in the pathogenesis of pancreatic exocrine insufficiency.

In this study we also demonstrate that after 7 days of treatment with an LXR agonist (T2320), mRNA levels of AQP-1 are

significantly increased in WT mice. Low AQP-1 gene expression in LXR$\beta^{-/-}$ mice and the increased expression after LXR agonist treatment support the idea that AQP-1 is regulated by LXRβ transcriptional activity in the pancreas. Little is known about the transcriptional regulation of the AQP-1 gene. In epithelial cells of the ventricular choroid plexus, the AQP-1 gene is regulated by thyroid transcription factor-1 (TTF-1), (30), and in efferent ducts of epididymis (31, 32) it is estrogen-regulated. It is not known whether LXRβ binds directly to the promoter of AQP-1; the AQP-1 5′ flank has multiple LXRE half sites, and further studies are required to analyze whether any of them is functional.

Although immunohistochemical studies in humans have demonstrated the presence of AQP-1 in the intralobular and interlobular pancreatic ducts, nothing is known about the relations between pancreatic exocrine insufficiency, malabsorption, and lack of expression of AQP-1. More studies are required to clarify the regulatory pathway of LXRβ-AQP-1 in human pathophysiology and determine whether LXRβ can be used as a target in the treatment of diseases associated with a dysregulation of the gastrointestinal fluid balance such as in pancreatic insufficiency and cystic fibrosis.

Materials and Methods

Animals. Mice of WT, LXR$\alpha^{-/-}$, LXR$\beta^{-/-}$, and LXR$\alpha^{-/-}\beta^{-/-}$ genotypes were generated as described (10). Mice used in this study were back-crossed to C57BL/6 mice for at least 10 generations and were maintained on a 12-h light/dark cycle under controlled temperature (20–22°C) and humidity (50–65%) in the Karolinska University Hospital Animal Facility (Huddinge, Sweden). Animals were given free access to tap water and standard chow diet (RM3; Scanbur Bk) containing 15.15 MJ/kg of gross energy. The quantity of food and the body weight were measured daily for 7 days when mice were 11 months of age. Naso-anal length was determined after death, by pushing the back of the mouse flat with straightened spine by using a digital caliper.

Experiments were approved by the local ethical committee for animal experiments, and the guidelines for the care and use of laboratory animals were followed.

Tissue Processing. Mice were killed by CO_2 asphyxiation, and blood was drawn by intracardiac puncture for subsequent serum collection. Pancreas was removed and fixed overnight in 4% paraformaldehyde at 4°C for immunohistochemical studies or frozen in liquid nitrogen for Western blotting and RT-PCR.

Serum α-Amylase and Lipase Assay. Levels of α-amylase and lipase in serum were measured with a QuantiChrom Lipase assay kit (DLPS-100; BioAssay Systems) and a QuantiChrom α-Amylase assay kit (DAMY-100; BioAssay Systems) according to the manufacturer's instructions.

Measurement of Total Proteases in Mouse Feces. Fresh feces of WT, LXR$\alpha^{-/-}$, LXR$\beta^{-/-}$, and LXR$\alpha^{-/-}\beta^{-/-}$ mice were collected and stored at −20°C. Samples of 10 mg were suspended in 1 ml of solvent (0.1% Triton X-100, 0.5 M NaCl, and 100 mM $CaCl_2$), sonicated, and centrifuged at 40,000 × *g* for 10 min at 4°C as described (33). The supernatant (0.2 ml) was incubated with 3% Azo-Casein (Fluka 11610) dissolved in 50 mM Tris·HCl buffer, pH 8.5 at 37°C for 60 min. After stopping the reaction by the addition of 0.5 ml of 8% trichloroacetic acid, the solution was centrifuged at 9,500 × *g* for 5 min. The supernatant was subjected to absorbance measurement at 366 nm by using a spectrophotometer (Molecular Devices Spectra Max 250) at room temperature as described (34). All assays were done in triplicate.

Standard curve was done by using different concentrations of trypsin standard (Promega V511A). Activity was expressed as units/mg feces.

Evaluation of Cell Death and Proliferation. To identify apoptosis, TUNEL was performed by using an *in situ* cell death detection kit (Roche) according to the manufacturer's specifications for paraffin-embedded tissues. Pancreatic duct proliferation was evaluated in WT and LXR$\beta^{-/-}$ male mice, treated i.p. with BrdU (Roche) dissolved in 0.9% of NaCl at 100 mg/kg every 12 h for 3 days (total of six injections).

Generation of Antibody Against LXRβ. Goat polyclonal LXRβ-946 antibody was directed against the N-terminal region of mouse LXRβ-946 amino acids 1–17.

Preadsorption of LXRβ Antibody. A total of 0.2 g of CNBr-activated Sepharose (Amersham Bioscience) was added to 10 ml of 0.1 M HCl and washed on a funnel with 200 ml of 0.1 M HCl.

LXRβ protein (3 mg/ml) (35) was coupled to Sepharose in 5 ml of sodium bicarbonate for 12 h at 4°C on a wheel. After centrifugation (9,500 × *g* for 5 min), the pellet was incubated with LXRβ IgG (1:100 in PBS) for 12 h at 4°C on a wheel. After centrifugation for 5 min at 9,500 × *g*, the supernatant was used for immunohistochemical staining. As control for preadsorption experiments, BSA was coupled to activated Sepharose.

Immunohistochemistry. Representative blocks of paraffin-embedded tissues were cut at 4-μm thickness, dewaxed in xylene, and rehydrated through graded ethanol. Antigens were retrieved by boiling 10 mM citrate buffer (pH 6.0) for 5 min. Cooled sections were incubated in 3% H_2O_2 in 50% methanol for 30 min at room temperature to quench endogenous peroxidase, and then incubated in 0.5% Triton X-100 in PBS for 10 min. For BrdU staining, before Triton X-100 incubation, sections were incubated in 2 M hydrochloric acid for 10 min, followed by incubation for 15 min at room temperature in a solution of 0.05 M NaCl and 0.05 M sodium tetraborate (pH 8.5) in 0.2 M boric acid. To block nonspecific binding, sections were incubated in PBS containing 1% BSA and 0.1% Nonidet P-40 for 1 h at 4°C. Sections were incubated with the following antibodies: anti-LXRβ (1:100), anti-BrdU (1:100; Biosciences Pharmingen), anti-AQP1 (1:100; Alpha Diagnostic International) in PBS containing 1% BSA and 0.1% Nonidet P-40 overnight at 4°C. Negative controls were incubated with PBS containing 1% BSA and 0.1% Nonidet P-40 without primary antibody. After washing, sections were incubated with the corresponding secondary antibodies (1:200; Zymed Laboratories), rabbit anti-goat IgG for LXRβ staining, goat anti-mouse IgG for BrdU staining, and goat anti-rabbit for AQP1 staining at room temperature for 1 h. The Vectastain ABC kit (Vector Laboratories) was used for the avidin-biotin complex method to visualize the signal, following the manufacturer's instructions. After washing in PBS, sections were developed with 3,3′-diaminobenzidine tetrahydrochloride substrate (DAKO). A light counterstaining with Mayer's hematoxylin was done. Sections were dehydrated through a graded ethanol series and xylene and then mounted.

Western Blotting. Pancreatic nuclear fractions from WT, LXR$\beta^{-/-}$, and LXR$\alpha^{-/-}\beta^{-/-}$ mice were analyzed by Western blotting. Frozen pancreatic tissues were homogenized for 1 min each with a Polytron in 25 ml of PBS containing protease inhibitor mixture according to the supplier's instructions (Roche Diagnostics). The protein content was measured by Bio-Rad protein assay with BSA as standard. Twenty micrograms of protein was dissolved in SDS sample buffer and resolved on 4–20% gradient SDS/polyacrylamide gels (Invitrogen) in Tris-glycine buffer. Proteins were transferred to PVDF membranes (Amersham Pharmacia Biosciences) by electroblotting in Tris·glycine buffer. Molecular weight markers were PageRuler Prestained Protein Ladder Plus (Fermentas). The membrane was then incubated in blocking solution containing 3% BSA and 0.1% Nonidet P-40 in PBS for 1 h at room temperature. Incubation with goat anti-LXRβ (1:5,000) was performed in blocking solution overnight at 4°C. For positive control, LXRβ protein was used (35). After washing, secondary peroxidase-conjugated donkey anti-goat antibody (1:10,000; Santa Cruz Biotechnology) was applied in blocking solution for 1 h at room temperature. After washing, detection with an enhanced chemiluminescence kit (Amersham Pharmacia) was performed.

Transmission Electron Microscopy. Pancreas was dissected, and small pieces were immediately fixed in 2% glutaraldehyde + 0.5% paraformaldehyde in 0.1 M sodium cacodylate buffer containing 0.1 M sucrose and 3 mM $CaCl_2$, pH 7.4, at room temperature and stored at 4°C until further processing. Specimens were rinsed in 0.15 M sodium cacodylate buffer containing 3 mM $CaCl_2$, pH 7.4, postfixed in 2% osmium tetroxide in 0.07 M sodium cacodylate buffer containing 1.5 mM $CaCl_2$, pH 7.4 at 4°C for 2 h, dehydrated in ethanol followed by acetone, and embedded in LX-112 (Ladd). Semithin sections were cut and stained with toluidine blue and used for light microscopic analysis. Ultrathin sections (≈40–50 nm) were cut and contrasted with uranyl acetate followed by lead citrate and examined in a Leo 906 transmission electron microscope at 80 kV. Digital images were taken with a Morada digital camera (Soft Imaging System) (36).

LXR Agonist Treatment. Five male C57B16/J mice, 8 months of age, were treated with 20 mg/kg body weight of LXR agonist T0901317 (T2320 Sigma–Aldrich), dissolved in DMSO/PBS (1:3), given daily by oral gavage for 7 days. Six mice were given only vehicle for 7 days.

Real-Time RT-PCR. Total RNA was extracted from frozen pancreas tissues by using the RNeasy Mini KIT (Qiagen) following the manufacturer's instructions. One microgram of RNA was treated with RNase-Free DNase Set (Qiagen), and then reverse-transcribed with 100 ng of random hexamer primer by using SuperScript III reverse transcriptase (Invitrogen). All genes were analyzed with the SYBR green detection method by using the Applied Biosystems 7500 real-time PCR machine. The forward and reverse primer sequences were obtained from published studies (37, 38). Each PCR was run in duplicate with two different cDNA templates. β-Actin was used as internal control for each of the PCR amplifications.

Statistical Analyses. Data were expressed as mean $\pm$ SE, and Student's *t* test was used to analyze individual differences. A value of $P < 0.05$ was considered to be statistically significant. Statistical analysis was performed with SPSS statistical software (version 15.0 for Windows).

ACKNOWLEDGMENTS. We thank Rodrigo Barros for very helpful discussions and Christina Tulin Andersson for excellent technical assistance and Western blotting experiments. This study was supported by grants from the Swedish Science Council, KaroBio AB, and the European Union Integrated Project CRESCENDO.

1. Owens SR, Greenson JK (2007) The pathology of malabsorption: Current concepts. *Histopathology* 50:64–82.
2. Witt H (2003) Chronic pancreatitis and cystic fibrosis. *Gut* 52 Suppl 2:ii31–41.
3. Witt H, Apte MV, Keim V, Wilson JS (2007) Chronic pancreatitis: Challenges and advances in pathogenesis, genetics, diagnosis, and therapy. *Gastroenterology* 132:1557–1573.
4. Balog A, *et al.* (2005) Polymorphism of the TNF-α, HSP70–2, and CD14 genes increases susceptibility to severe acute pancreatitis. *Pancreas* 30:e46–e50.
5. Janowski BA, *et al.* (1999) Structural requirements of ligands for the oxysterol liver X receptors LXRα and LXRβ. *Proc Natl Acad Sci USA* 96:266–271.
6. Mitro N, *et al.* (2007) The nuclear receptor LXR is a glucose sensor. *Nature* 445:219–223.
7. Kainu T, Kononen J, Enmark E, Gustafsson JA, Pelto-Huikko M (1996) Localization and ontogeny of the orphan receptor OR-1 in the rat brain. *J Mol Neurosci* 7:29–39.
8. Zhang Y, Mangelsdorf DJ (2002) LuXuRies of lipid homeostasis: The unity of nuclear hormone receptors, transcription regulation, and cholesterol sensing. *Mol Interv* 2:78–87.
9. Zelcer N, Tontonoz P (2006) Liver X receptors as integrators of metabolic and inflammatory signaling. *J Clin Invest* 116:607–614.
10. Alberti S, *et al.* (2001) Hepatic cholesterol metabolism and resistance to dietary cholesterol in LXRβ-deficient mice. *J Clin Invest* 107:565–573.
11. Peet DJ, *et al.* (1998) Cholesterol and bile acid metabolism are impaired in mice lacking the nuclear oxysterol receptor LXRα. *Cell* 93:693–704.
12. Gerin I, *et al.* (2005) LXRβ is required for adipocyte growth, glucose homeostasis, and β-cell function. *J Biol Chem* 280:23024–23031.
13. Kalaany NY, *et al.* (2005) LXRs regulate the balance between fat storage and oxidation. *Cell Metab* 1:231–244.
14. Ectors N, *et al.* (1997) Nonalcoholic duct destructive chronic pancreatitis. *Gut* 41:263–268.
15. Esrefoglu M, Gul M, Ates B, Selimoglu MA (2006) Ultrastructural clues for the protective effect of melatonin against oxidative damage in cerulein-induced pancreatitis. *J Pineal Res* 40:92–97.
16. Nielsen S, Smith BL, Christensen EI, Agre P (1993) Distribution of the aquaporin CHIP in secretory and resorptive epithelia and capillary endothelia. *Proc Natl Acad Sci USA* 90:7275–7279.
17. Preston GM, Carroll TP, Guggino WB, Agre P (1992) Appearance of water channels in *Xenopus* oocytes expressing red cell CHIP28 protein. *Science* 256:385–387.
18. Roberts SK, *et al.* (1994) Cholangiocytes express the aquaporin CHIP and transport water via a channel-mediated mechanism. *Proc Natl Acad Sci USA* 91:13009–13013.
19. Calamita G, *et al.* (2005) Expression and subcellular localization of the AQP8 and AQP1 water channels in the mouse gall-bladder epithelium. *Biol Cell* 97:415–423.
20. Furuya S, *et al.* (2002) Distribution of aquaporin 1 in the rat pancreatic duct system examined with light- and electron-microscopic immunohistochemistry. *Cell Tissue Res* 308:75–86.
21. Ma T, *et al.* (1998) Severely impaired urinary concentrating ability in transgenic mice lacking aquaporin-1 water channels. *J Biol Chem* 273:4296–4299.
22. Schnermann J, *et al.* (1998) Defective proximal tubular fluid reabsorption in transgenic aquaporin-1 null mice. *Proc Natl Acad Sci USA* 95:9660–9664.
23. Oshio K, Watanabe H, Song Y, Verkman AS, Manley GT (2005) Reduced cerebrospinal fluid production and intracranial pressure in mice lacking choroid plexus water channel aquaporin-1. *FASEB J* 19:76–78.
24. Saadoun S, Papadopoulos MC, Hara-Chikuma M, Verkman AS (2005) Impairment of angiogenesis and cell migration by targeted aquaporin-1 gene disruption. *Nature* 434:786–792.
25. Thiagarajah JR, Verkman AS (2002) Aquaporin deletion in mice reduces corneal water permeability and delays restoration of transparency after swelling. *J Biol Chem* 277:19139–19144.
26. Ma T, *et al.* (2001) Defective dietary fat processing in transgenic mice lacking aquaporin-1 water channels. *Am J Physiol* 280:C126–C134.
27. Arnaoutova I, *et al.* (2008) Aquaporin 1 is important for maintaining secretory granule biogenesis in endocrine cells. *Mol Endocrinol* 22:1924–1934.
28. Cho SJ, *et al.* (2002) Aquaporin 1 regulates GTP-induced rapid gating of water in secretory vesicles. *Proc Natl Acad Sci USA* 99:4720–4724.
29. Jeremic A, Cho WJ, Jena BP (2005) Involvement of water channels in synaptic vesicle swelling. *Exp Biol Med (Maywood)* 230:674–680.
30. Kim JG, *et al.* (2007) Thyroid transcription factor-1 facilitates cerebrospinal fluid formation by regulating aquaporin-1 synthesis in the brain. *J Biol Chem* 282:14923–14931.
31. Fisher JS, *et al.* (1998) Immunoexpression of aquaporin-1 in the efferent ducts of the rat and marmoset monkey during development, its modulation by estrogens, and its possible role in fluid resorption. *Endocrinology* 139:3935–3945.
32. Oliveira CA, Carnes K, Franca LR, Hermo L, Hess RA (2005) Aquaporin-1 and -9 are differentially regulated by oestrogen in the efferent ductule epithelium and initial segment of the epididymis. *Biol Cell* 97:385–395.
33. Zenker M, *et al.* (2005) Deficiency of UBR1, a ubiquitin ligase of the N-end rule pathway, causes pancreatic dysfunction, malformations and mental retardation (Johanson-Blizzard syndrome). *Nat Genet* 37:1345–1350.
34. Dahlmann B, Reinauer H (1978) Purification and some properties of an alkaline proteinase from rat skeletal muscle. *Biochem J* 171:803–810.
35. Toresson G, *et al.* (2004) Purification of functional full-length liver X receptor β produced in *Escherichia coli*. *Protein Expression Purif* 35:190–198.
36. Park CB, *et al.* (2007) MTERF3 is a negative regulator of mammalian mtDNA transcription. *Cell* 130:273–285.
37. Danyu L, Ying L, Zhenwu B, Heming Y, Xuejun L (2008) Aquaporin 1 expression in the testis, epididymis, and vas deferens of postnatal ICR mice. *Cell Biol Int* 32:532–541.
38. Williamson MA, Gasiewicz TA, Opanashuk LA (2005) Aryl hydrocarbon receptor expression and activity in cerebellar granule neuroblasts: Implications for development and dioxin neurotoxicity. *Toxicol Sci* 83:340–348.